Inorganic Chemistry
Communication

Inorg. Chem. **2011**, *50*, 421–423 **421**
DOI: 10.1021/ic102378u

$Mn_{21}Dy$ Cluster with a Record Magnetization Reversal Barrier for a Mixed 3d/4f Single-Molecule Magnet

Constantina Papatriantafyllopoulou,[†] Wolfgang Wernsdorfer,[‡] Khalil A. Abboud,[†] and George Christou*,[†]

[†]*Department of Chemistry, University of Florida, Gainesville, Florida 32611-7200, United States, and*
[‡]*Institut Louis Néel, CNRS/UJF, BP 166, 38042 Grenoble Cedex 9, France*

Received November 29, 2010

A high-oxidation-state $Mn^{III,IV}_{21}Dy^{III}$ cluster with an unusual structure is reported. It also possesses a record barrier to magnetization reversal for a 3d/4f single-molecule magnet (SMM) and provides insight into how the full benefit of lanthanides to the mixed 3d/4f SMM field might be realized.

Single-molecule magnets (SMMs) are individual molecules that function as single-domain nanoscale magnets and thus represent a molecular approach to nanomagnetism.[1,2] They derive their properties from a large ground-state spin (S) and easy-axis magnetoanisotropy (negative zero-field-splitting parameter, D), which result in hysteresis in magnetization versus applied field scans below a characteristic blocking temperature, T_B. The upper limit to the relaxation barrier (U) is $S^2|D|$ or $(S^2 - {}^1/_4)|D|$ for integer and half-integer spins, respectively; in practice, quantum tunneling of the magnetization (QTM)[3] makes the true (effective) barrier (U_{eff}) less than U.

One strategy to new SMMs has been mixed 3d/4f chemistry, particularly Mn/Ln (Ln = lanthanide), seeking to amalgamate the propensity of Mn_x clusters to possess large spin S values with the much larger anisotropies of many Ln ions. The first 3d/4f SMM was a Cu_2Tb_2 complex in 2004[4] and the first Mn/Ln SMM a Mn_6Dy_6 complex that same year.[5] Also in 2004 were reported $Mn_{11}Ln_4$ SMMs,[6] exhibiting hysteresis and QTM. Many other Mn/Ln SMMs have subsequently been reported, including $Mn_{12}Gd$,[7] $Mn_{11}Ln_2$,[8a] Mn_5Ln_4,[8b] Mn_9Dy_8,[8c] Mn_4Ln_4,[8d] Mn_2Ln_2,[8e,f] and Mn_4Ln_3[8g] examples. It is interesting that, despite this growing family of Mn/Ln SMMs, the highest U_{eff} is 38.6 K for a Mn_5Dy_4,[8b] a factor of 2 below those of the homometallic Mn_6 (86.4 K)[9a] and Mn_{12} (70−76 K) SMMs,[9b] even though homometallic Ln_x SMMs have displayed very large U_{eff} values,[10] with up to 641 cm^{-1} having been reported.[10e] The low barriers of 3d/4f SMMs are likely due to low-energy relaxation pathways resulting from low-lying excited states due to the weak exchange interactions characteristic of 3d/4f couplings.[11]

We recently described a $Mn_{12}Gd$ complex with a high O^{2-}/M ratio of 9:13 and a large number (eight) of O^{2-} ions bridging between Gd and Mn.[7] Because O^{2-} ions are good

*To whom correspondence should be addressed. E-mail: christou@chem.ufl.edu.

(1) (a) Sessoli, R.; Gatteschi, D.; Hendrickson, D. N.; Christou, G. *MRS Bull.* **2000**, *25*, 66. (b) Lis, T. *Acta Crystallogr., Sect. B* **1980**, *36*, 2042. (c) Sessoli, R.; Tsai, H.-L.; Schake, A. R.; Wang, S.; Vincent, J. B.; Folting, K.; Gatteschi, D.; Christou, G.; Hendrickson, D. N. *J. Am. Chem. Soc.* **1993**, *115*, 1804. (d) Sessoli, R.; Gatteschi, D.; Caneschi, A.; Novak, M. A. *Nature* **1993**, *365*, 141.

(2) (a) Bagai, R.; Christou, G. *Chem. Soc. Rev.* **2009**, *38*, 1011 and references cited therein. (b) Aromi, G.; Brechin, E. K. *Struct. Bonding* (*Berlin*) **2006**, *122*, 1.

(3) (a) Friedman, J. R.; Sarachik, M. P.; Tejada, J.; Ziolo, R. *Phys. Rev. Lett.* **1996**, *76*, 3830. (b) Thomas, L.; Lionti, L.; Ballou, R.; Gatteschi, D.; Sessoli, R.; Barbara, B. *Nature* **1996**, *383*, 145.

(4) Osa, S.; Kido, T.; Matsumoto, N.; Re, N.; Pochaba, A.; Mrozinski, J. *J. Am. Chem. Soc.* **2004**, *126*, 420.

(5) Zaleski, C. M.; Depperman, E. C.; Kampf, J. W.; Kirk, M.-L.; Pecoraro, V. L. *Angew. Chem., Int. Ed.* **2004**, *43*, 3912.

(6) Mishra, A.; Wernsdorfer, W.; Abboud, K. A.; Christou, G. *J. Am. Chem. Soc.* **2004**, *126*, 15648.

(7) Stamatatos, T. C.; Teat, S. J.; Wernsdorfer, W.; Christou, G. *Angew. Chem., Int. Ed.* **2009**, *48*, 521.

(8) (a) Mereacre, V.; Ako, A. M.; Clerac, R.; Wernsdorfer, W.; Filoti, G.; Bartolome, J.; Anson, C. E.; Powell, A. K. *J. Am. Chem. Soc.* **2007**, *129*, 9248. (b) Mereacre, V.; Ako, A. M.; Clerac, R.; Wernsdorfer, W.; Hewitt, I. J.; Anson, C. E.; Powell, A. K. *Chem.—Eur. J.* **2008**, *14*, 3577. (c) Langley, S.; Moubaraki, B.; Murray, K. S. *Dalton Trans.* **2010**, *39*, 5066. (d) Karotsis, G.; Kennedy, S.; Teat, S. J.; Beavers, C. M.; Fowler, D. A.; Morales, J. J.; Evangelisti, M.; Dalgarno, S. J.; Brechin, E. K. *J. Am. Chem. Soc.* **2009**, *132*, 12983. (e) Mereacre, V.; Lan, Y.; Clerac, R.; Ako, A. M.; Hewitt, I. J.; Wernsdorfer, W.; Buth, G.; Anson, C. E.; Powell, A. K. *Inorg. Chem.* **2010**, *49*, 5293. (f) Mishra, A.; Wernsdorfer, W.; Parsons, S.; Christou, G.; Brechin, E. K. *Chem. Commun.* **2005**, 2086. (g) Liu, C.-M.; Zhang, D.-Q.; Zhu, D.-B. *Dalton Trans.* **2010**, *39*, 11325.

(9) (a) Milios, C. J.; Inglis, R.; Vinslava, A.; Bagai, R.; Wernsdorfer, W.; Parsons, S.; Perlepes, S. P.; Christou, G.; Brechin, E. K. *J. Am. Chem. Soc.* **2007**, *129*, 12505. (b) Redler, G.; Lampropoulos, C.; Datta, S.; Koo, C.; Stamatatos, T. C.; Chakov, N. E.; Christou, G.; Hill, S. *Phys. Rev. B* **2009**, *80*, 094408-1–094408-9.

(10) (a) Ishikawa, N.; Sugita, M.; Ishikawa, T.; Koshihara, S.-Y.; Kaizu, Y. *J. Am. Chem. Soc.* **2003**, *125*, 8694. (b) Ishikawa, N.; Sugita, M.; Ishikawa, T.; Koshihara, S.; Kaizu, Y. *J. Phys. Chem. B* **2004**, *108*, 11265. (c) Ishikawa, N.; Sugita, M.; Wernsdorfer, W. *Angew. Chem., Int. Ed.* **2005**, *44*, 2931. (d) Lin, P.-H.; Burchell, T. J.; Liviu, U.; Chibotaru, L. F.; Wernsdorfer, W.; Murugesu, M. *Angew. Chem., Int. Ed.* **2009**, *48*, 1. (e) Branzoli, F.; Carretta, P.; Filibian, M.; Zoppellaro, G.; Graf, M. J.; Galan-Mascaros, J. R.; Fuhr, O.; Brink, S.; Ruben, M. *J. Am. Chem. Soc.* **2009**, *131*, 4387.

(11) (a) Mori, F.; Nyui, T.; Ishida, T.; Nogami, T.; Choi, K.-Y.; Nojiri, H. *J. Am. Chem. Soc.* **2006**, *128*, 1440. (b) Okazawa, A.; Nogami, T.; Nojiri, H.; Ishida, T. *Inorg. Chem.* **2008**, *47*, 9763. (c) Costes, J.-P.; Dahan, F.; Dupuis, A.; Laurent, J.-P. *Chem.—Eur. J.* **1998**, *4*, 1616. (d) Lampropoulos, C.; Stamatatos, T. C.; Abboud, K. A.; Christou, G. *Inorg. Chem.* **2009**, *48*, 429.

Published on Web 12/13/2010

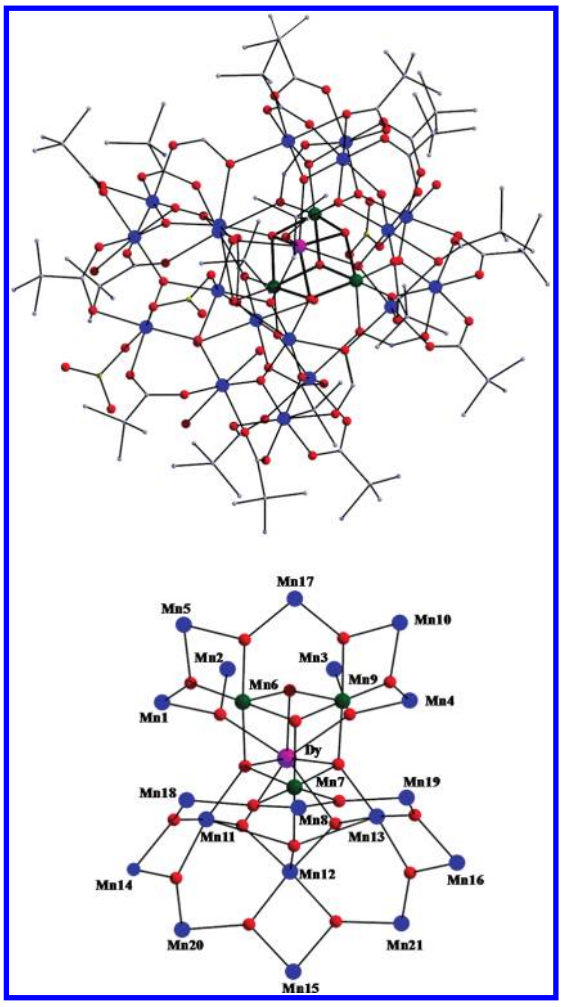

Figure 1. Molecular structures of **1** (top) and its $[Mn_{21}DyO_{20}]$ core (bottom). H atoms have been omitted for clarity. Color code: Mn^{III}, blue; Mn^{IV}, green; Dy, purple; O, red; N, yellow; C, gray.

mediators of exchange interactions, the coupling of Gd to the Mn_x shell was likely stronger than usual (but still weak in an absolute sense) because alternating-current (ac) susceptibility data indicated only the ground state to be populated below ~5 K. This suggested that a complex with a large S, anisotropic Ln^{III} atoms(s), and an even higher O^{2-}/M ratio might possess an equally or better isolated ground state and perhaps a significantly increased barrier. To thus encourage a greater oxide content and higher O^{2-}/M ratios, we have been targeting higher oxidation state Mn^{III}/Mn^{IV} products by including MnO_4^- as a reagent. We can now report a $Mn_{21}Dy$ cluster with an enhanced anisotropy barrier comparable to that of the Mn_{12} SMMs.

The reaction of $Mn(NO_3)_2 \cdot 6H_2O$, $Dy(NO_3)_3 \cdot 6H_2O$, $NBu^n_4MnO_4$, Bu^tCO_2H, and HCO_2H (4:4:1:32:1) in $MeNO_2$ gave $[Mn_{21}DyO_{20}(OH)_2(Bu^tCO_2)_{20}(HCO_2)_4(NO_3)_3(H_2O)_7]$ (**1**) as dark-red crystals of $\mathbf{1} \cdot 5MeNO_2 \cdot H_2O$ in 25% yield. The structure[12] consists of a $[Mn^{IV}_3Mn^{III}_{18}Dy(\mu_4\text{-}O^{2-})_2(\mu_3\text{-}O^{2-})_{18}]$ core (Figure 1) comprising a $[DyMn^{IV}_3O_4]^{7+}$ cubane, on top of which is attached by oxide ions a nonplanar Mn_7 loop and on the bottom of which is a nonplanar Mn_8 loop, as

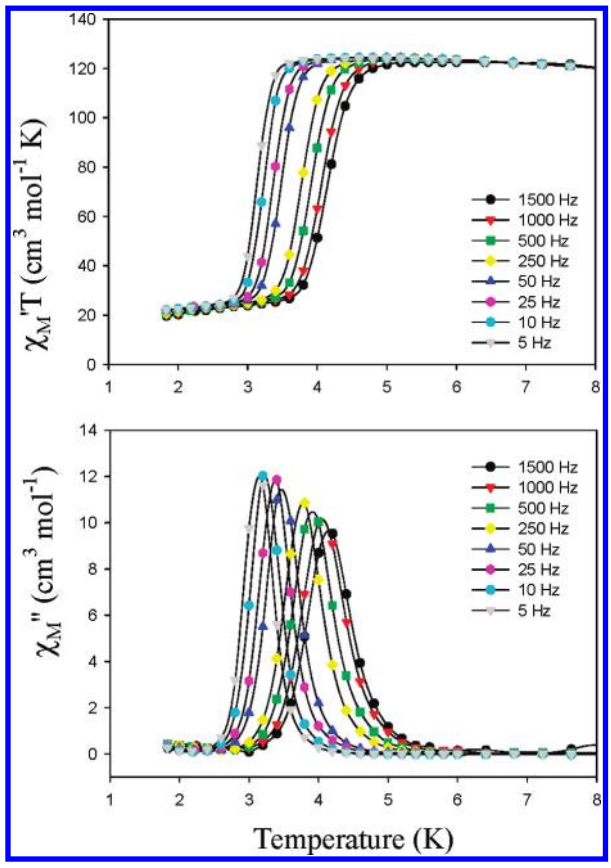

Figure 2. Plot of (top) the in-phase (χ_M', as $\chi_M'T$) and (bottom) out-of-phase (χ_M'') ac susceptibility signals for complex **1** in a 3.5 Oe field oscillating at the indicated frequencies.

well as additional Mn atoms (Mn11, Mn12, and Mn13); the total O^{2-}/M ratio is 20:22, much higher than that for the $Mn_{12}Gd$ SMM. Peripheral ligation is by 3 μ_3- and 17 μ-pivalates, 4 μ_3-formates, 2 μ-OH^- ions, 1 μ-NO_3^- and 2 monodentate NO_3^- groups, and 7 terminal water molecules. Metal oxidation states and O^{2-}/OH^- protonation levels were established by bond-valence-sum (BVS) calculations.[13] Mn atoms are all six-coordinate, except five-coordinate Mn11 and Mn13, and the Dy^{III} atom is eight-coordinate, bound to seven O^{2-} ions and a terminal O atom (O3) of a μ_3-pivalate. There are several intramolecular O−H···O hydrogen bonds but no intermolecular ones, and each molecule is thus essentially magnetically isolated from its neighbors. Complex **1** is the highest-nuclearity Mn/Ln cluster to date.

Solid-state direct-current (dc) magnetic susceptibility (χ_M) data were collected in the 5−300 K range in a 1000 Oe field (Figure S1 in the Supporting Information, SI).[14] $\chi_M T$ is 69.73 cm^3 mol^{-1} K at 300 K, decreasing slightly with decreasing temperature to 64.37 cm^3 mol^{-1} K at 100 K, and then increasing sharply to 119.10 cm^3 mol^{-1} K at 5 K, suggesting a large ground-state spin. To investigate whether **1** is an SMM, ac susceptibility data were collected. The in-phase $\chi_M'T$ (Figure 2, top) is a plateau below ~6 K, indicating a well-isolated ground state. At lower T, there is a frequency-dependent decrease in $\chi_M'T$ and a concomitant out-of-phase

(12) Crystal structure data for $\mathbf{1} \cdot 5MeNO_2 \cdot H_2O$: $C_{104}H_{204}O_{88}N_3Mn_{21}Dy$ (without solvate molecules), M_w = 4184.91, monoclinic, $P2_1$, a = 19.1503(4) Å, b = 19.7093(4) Å, c = 26.1294(6) Å, β = 111.4940(10)°, V = 9176.4(3) Å^3, T = 100(2) K, Z = 2, d_{calc} = 1.515 g cm^{-3}, R1 = 0.0518, wR2 = 0.0816.

(13) (a) BVS calculations gave 2.82−3.04 for Mn^{3+} ions, 3.91−3.96 for Mn^{4+} ions, 0.80 and 1.06 for OH^- ions, and 1.77−2.07 for O^{2-} ions. (b) Liu, W.; Thorp, H.-H. *Inorg. Chem.* **1993**, *32*, 4102. (c) Brown, I. D.; Altermatt, D. *Acta Crystallogr., Sect. B* **1985**, 244.

(14) See the Supporting Information.

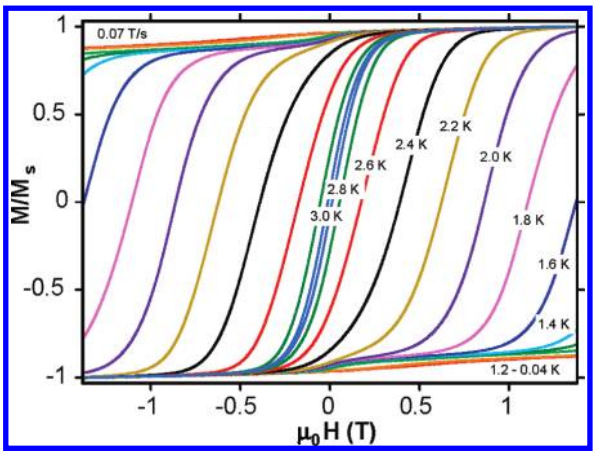

Figure 3. Magnetization (M) vs dc field (H) hysteresis loops for single crystals of $1\cdot 5MeNO_2\cdot H_2O$ at the indicated temperatures. The magnetization is normalized to its saturation value (M_s).

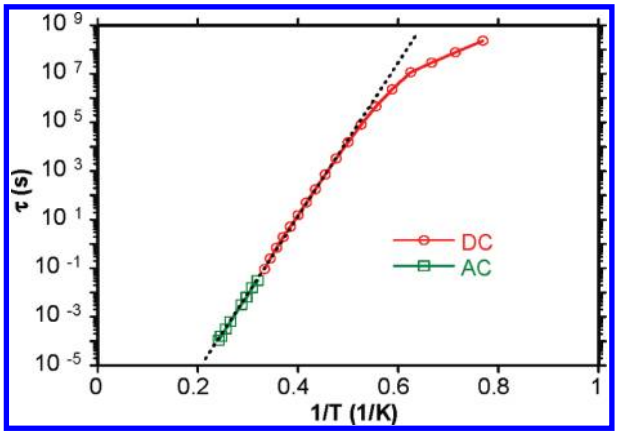

Figure 4. Plot of the relaxation time (τ) versus $1/T$ using ac χ_M'' and dc magnetization decay data for $1\cdot 5MeNO_2\cdot H_2O$. The dashed line is the fit of the thermally activated region to the Arrhenius equation. See the text for the fit parameters.

(χ_M'') signal (Figure 2, bottom), indicative of an SMM. **1** was confirmed as an SMM by magnetization versus dc field scans on single crystals of $1\cdot 5MeNO_2\cdot H_2O$ using a micro-SQUID;[15] hysteresis loops were seen at $\leq$3.0 K, whose coercivities increase with decreasing temperature (Figure 3) and increasing field sweep rate (Figure S2 in the SI),[14] as expected for an SMM.

Relaxation time (τ) versus T data obtained from the χ_M'' versus T data were combined with those at lower temperatures from dc magnetization decay versus time studies (Figure S3 in the SI) and used to construct an Arrhenius plot based on eq 1 (Figure 4)

$$\tau = \tau_0 \exp(U_{eff}/kT) \quad (1)$$

where U_{eff} is the effective barrier to magnetization relaxation and τ_0 is the preexponential factor. A fit of the thermally activated region gave $U_{eff} = 74$ K and $\tau_0 = 2.0 \times 10^{-12}$ s. U_{eff} is approximately double the previous record for a Mn/Ln SMM[9b] and comparable to those of the Mn_{12} family (70−76 K). τ_0 is smaller than usual for smaller SMMs, but such values are commonly encountered for high-nuclearity SMMs.[16]

(15) Wernsdorfer, W. *Adv. Chem. Phys.* **2001**, *118*, 99.

Extension of the work to other Ln^{III} analogues of **1** has been initiated. To factor out the effect of the Dy^{III} anisotropy (free ion $S = {}^5/_2$, $L = 5$, and ${}^6H_{15/2}$) on the properties of **1**, the isotropic Gd analogue (**2**) has been prepared by the same method. The ac in-phase ($\chi_M'T$) and out-of-phase (χ_M'') versus T data (Figure S4 in the SI)[14] reveal that this compound is also an SMM with a well-isolated ground state of appreciable spin. The latter was determined by $M/N\mu_B$ versus H/T fits using magnetization (M) data collected in the 0.1−5 T and 1.8−10.0 K ranges (Figure S5 in the SI).[14] The fit was by matrix diagonalization to a model that assumes that only the ground state is populated, includes axial zero-field splitting ($D\hat{S}_z^2$) and the Zeeman interaction, and incorporates a full powder average. The fit (solid lines in Figure S5 in the SI) gave $S = 11$, $D = -0.258(3)$, and $g = 1.93(1)$. The upper limit ($U = S^2|D|$) to the barrier for **2** is thus 31.2 cm^{-1} (44.9 K), but the true barrier U_{eff} was found to be smaller at $U_{eff} = 27.6$ K from χ_M'' versus T data (Figure S6 in the SI). This is only ~38% that of **1**, clearly establishing the anisotropic Dy^{III} as the major contributor to the much higher barrier of $Mn_{21}Dy$ complex **1**.

Complex **1** does not display QTM steps in its hysteresis loops, but this is typical for almost all high-nuclearity SMMs whose QTM steps are smeared out by (i) a distribution of molecular environments, (ii) intermolecular interactions, and/or (iii) low-lying excited states. For **1**, the crystal structure and magnetism data rule out the last two possibilities, and the absence of steps is thus assigned to (i), consistent with the disordered solvate molecules in the gaps between molecules of **1** in the crystal.

In conclusion, Mn/Ln SMMs can possess barriers as high as the homometallic Mn_x SMMs if certain criteria are obeyed: a large spin and easy-axis anisotropy are necessary, of course, but in addition the Ln^{III} atom needs to be coupled as strongly as possible to the Mn_x array. In the present $Mn_{21}Dy$ SMM, this is by multiple bridging O^{2-} ions. In fact, not only is the O^{2-}/M ratio almost 1:1, but three of the Mn atoms coupled to Dy^{III} are Mn^{IV}, which are known to give stronger exchange couplings than Mn^{III}.[17] As a result, the ground state of **1** is well isolated, leading to a 3 K blocking temperature, the highest yet for a 3d/4f SMM. We are now (i) investigating the preparation of other $Mn_{21}Ln$ and $Mn_{21}Y$ analogues, to obtain the spin of the Mn_{21} subunit and to fully map out the variation in U_{eff} as a function of the Ln, and (ii) targeting analogues containing a second anisotropic Ln^{III} atom well coupled to the Mn_x array as a means of further increasing the anisotropy barrier.

Acknowledgment. This work was supported by NSF (Grant CHE-0910472) and the Cyprus Research Promotion Foundation (Grant DIETHNIS/STOXOS/0308/14).

Supporting Information Available: Crystallographic data (CIF format), the synthesis of **1** and its elemental analysis, and magnetic plots for **1** and **2**. This material is available free of charge via the Internet at http://pubs.acs.org.

(16) Stamatatos, T. C.; Nastopoulos, V.; Tasiopoulos, A. J.; Moushi, E. E.; Wernsdorfer, W.; Perlepes, S. P.; Christou, G. *Inorg. Chem.* **2008**, *47*, 10081.

(17) Stamatatos, T. C.; Christou, G. *Philos. Trans. R. Soc.* **2008**, *366*, 113.